Journal
www.biotechnology-journal.com

Research Article

Real-time pH monitoring of industrially relevant enzymatic reactions in a microfluidic side-entry reactor (μSER) shows potential for pH control

Pia Gruber[1], Marco P.C. Marques[1], Philipp Sulzer[2], Roland Wohlgemuth[3], Torsten Mayr[2], Frank Baganz[1] and Nicolas Szita[1]

[1] Department of Biochemical Engineering, University College London, Gordon Street, London, UK
[2] Institute of Analytical Chemistry and Food Chemistry, Graz University of Technology Graz, Austria
[3] Sigma–Aldrich, Member of Merck Group, Buchs, Switzerland

Monitoring and control of pH is essential for the control of reaction conditions and reaction progress for any biocatalytic or biotechnological process. Microfluidic enzymatic reactors are increasingly proposed for process development, however typically lack instrumentation, such as pH monitoring. We present a microfluidic side-entry reactor (μSER) and demonstrate for the first time real-time pH monitoring of the progression of an enzymatic reaction in a microfluidic reactor as a first step towards achieving pH control. Two different types of optical pH sensors were integrated at several positions in the reactor channel which enabled pH monitoring between pH 3.5 and pH 8.5, thus a broader range than typically reported. The sensors withstood the thermal bonding temperatures typical of microfluidic device fabrication. Additionally, fluidic inputs along the reaction channel were implemented to adjust the pH of the reaction. Time-course profiles of pH were recorded for a transketolase- and a penicillin G acylase-catalyzed reaction. Without pH adjustment, the former showed a pH increase of one pH unit and the latter a pH decrease of about 2.5 pH units. With pH adjustment, the pH drop of the penicillin G acylase-catalyzed reaction was significantly attenuated, the reaction condition kept at a pH suitable for the operation of the enzyme, and the product yield increased. This contribution represents a further step towards fully instrumented and controlled microfluidic reactors for biocatalytic process development.

Received	09 AUG 2016
Revised	16 JAN 2017
Accepted	18 JAN 2017
Accepted article online	20 JAN 2017

Supporting information available online

Keywords: Microreactor · Online monitoring · Optical sensor · Penicillin G acylase · pH sensor · Transketolase

1 Introduction

The effects of pH on the activity and stability of enzymes, ionization and stability of substrates, products and other components in the reaction mixture are fundamental to enzymatic reactions and belong to the historic foundations of biochemistry [1]. In enzymatic reaction systems involving the release or uptake of protons, it is especially important to monitor the pH to ensure efficient process control and to minimize changes in process yield and quality of the end product. Therefore, a robust pH monitoring method in real time is highly desirable to follow the progression of a reaction and, ultimately, to control it.

In conventional reactors, the pH can be monitored and controlled using pH electrodes in combination with feedback control systems that add acid or base to the reaction mixture (e.g. pH-stat titration) [2]. When down-scaling to reactors with operating volumes of millilitres and smaller, the integration of microelectrodes or any needle-type

Correspondence: Prof. Nicolas Szita, University College London, Biochemical Engineering, Bernard Katz Building, Gordon Street, London, WC1H 0AH, UK
E-mail: n.szita@ucl.ac.uk

Abbreviations: 6-APA, 6-amino benzyl penicillanic acid; **ERY,** L-erythrulose; **GA,** glycol aldehyde; **GC**, gas chromatography; **HPA,** hydroxyl pyruvate; **HPLC,** high performance liquid chromatography; **ISFET,** ion-sensitive field effect transistor; **PG,** penicillin G; **PGA,** penicillin G acylase; **TFA,** trifluoroacetic acid; **TK,** transketolase; **μSER,** microfluidic side-entry reactor

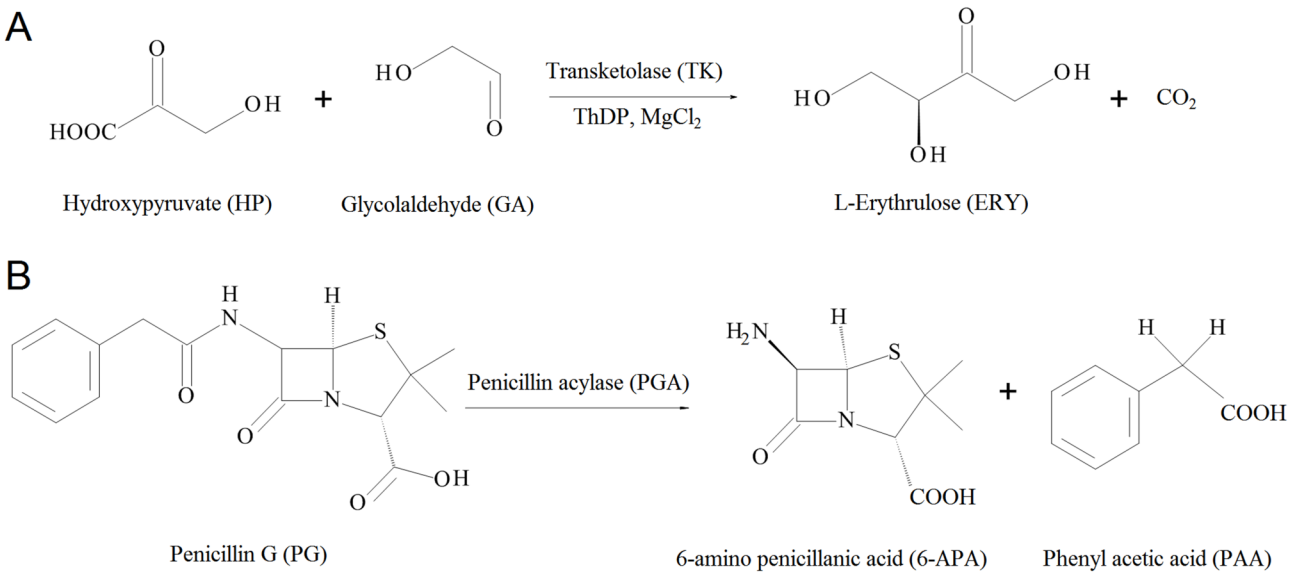

Scheme 1. Two enzyme-catalyzed reactions were studied in this research: (**A**) The transketolase (TK) catalyzed synthesis of L-erythrulose (ERY). (**B**) The penicillin G acylase (PGA) catalyzed formation of 6-amino penicillanic acid (6-APA) and phenyl acetic acid (PA). ThDP is thiamine pyrophosphate or thiamine diphosphate.

electrode becomes less practical. This integration challenge is exacerbated in microfluidic devices, where channels are normally small, narrow, and enclosed. Reactions can in principle be monitored at-line or off-line, for example with a HPLC or a GC; however, in reactions where a change in a common analyte such as oxygen or pH occurs, online monitoring is preferable, as it provides a direct, i.e. real time, measure of the progress of the reaction. On-line monitoring at the microfluidic scale thus enables the rapid analysis of enzymatic reactions with small amounts of enzymes, and – due to the fine control over the fluid flow afforded by microfluidics – with precise control over reaction conditions.

Monitoring of pH can be accomplished using electrochemical sensors, such as ion-sensitive field effect transistors (ISFETs) [3]. Since their first introduction as sensing tools they have found their way into microfluidics in the late 1990s [4], because of their low cost, fast response times and potential for miniaturization. And they have also been developed for monitoring pH and potassium [5]. Recently, Welch et al. [6] combined ISFETs and microfluidic valves to demonstrate controlled increase and decrease of pH in 0.14 pH increments inside a 90 nL chamber filled with a weak acid and a strong base, but the control of a reaction was not shown.

Optical sensors are more frequently applied in miniaturized and microfluidic devices than electrochemical sensors [7]. Optical pH sensors [8] were applied to observe a pH gradient in free-flow electrophoresis [9]; to detect pH in segments used for cell cultivation [10]; and to control the pH of microbial fermentations in a batch microbioreactor [11]. Recently, the potential for real-time pH monitoring of an enzymatic reaction in a microfluidic reactor was reported using novel pH sensors based on nanoparticles [12]. However, to date, on-line and real-time pH monitoring of the progression of an enzymatic reaction in a microfluidic reactor has not been reported. Additionally, most individual pH dyes typically only allow for robust and sensitive measurement over two to three pH units [13, 14], which constrains their application in process monitoring.

To establish and validate real-time pH monitoring in a microfluidic enzymatic reactor, well-defined biocatalytic reactions are required. We selected the transketolase-catalyzed synthesis of L-erythrulose (Scheme 1A) and the penicillin G acylase-catalyzed hydrolysis of penicillin G (Scheme 1B). Both of these involve a pH change during the reaction; a pH decrease in the penicillin acylase-catalyzed, and a pH increase in the transketolase-catalyzed reaction. Penicillin acylase is used for the production of 6-aminopenicillanic acid and β-lactam antibiotics [15–17]. It has also been used in peptide synthesis and for the resolution of racemic mixtures of chiral products [18]. Transketolase is a key enzyme in the non-oxidative branch of the pentose phosphate pathway and highly relevant. [19, 20]. The synthetic utility of transketolase-catalyzed reactions is based on the excellent selectivity and versatility of the two-carbon chain elongation of suitable aldehydes to more complex chiral compounds in combination with the irreversibility of this reaction by the use of hydroxypyruvate as carbon donor [21–25].

In this contribution, we demonstrate real-time monitoring of pH in a microfluidic reactor as a further step towards their use as novel process development tools for biocatalysis. To achieve this, optical pH sensor layers with dual lifetime referencing [26] were integrated in a microfluidic side-entry reactor. In contrast to nanosensor parti-

cles [12], monolithically integrated sensor layers are less prone to interact with sample, and do not have to be added to the sample in advance. We have previously shown the utility of microfluidic side-entry reactors (μSER) to improve the conversion yield of inhibition-prone enzyme reactions [27]. Here, we address the challenges of integrating optical sensors in narrow channels of thermally bonded microfluidic devices, and of their integration at multiple points in order to map the progression of an enzymatic reaction. To monitor a broad range of pH values, sensors with a detection range between pH 5 and pH 8.5 were complemented with novel sensors with a detection range between pH 3.5 and pH 6 [28]. Additionally, we demonstrate how the side entries of the side-entry reactor can be employed to adjust and balance the pH of enzymatic reactions, effectively leading to an increased reaction yield, which highlights the potential of a μSER for pH control.

2 Materials and methods

Unless specified otherwise, chemicals were purchased from Sigma Aldrich (Gillingham, UK) and were used without further purification.

2.1 Fabrication of the microfluidic side-entry reactor (μSER)

All components were designed using Solidworks® (Dassault Systems, Vélizy-Villacoublay, France). The reactor was comprised of two rigid 1.5 mm poly(methylmethacrylate) (PMMA) layers (RS Pro, Northants, United Kingdom). The channels and cut-outs were fabricated using a CO_2 laser marking head (Epilog Laser, Clevedon, UK) and the layers were thermally bonded (1 h, 110°C). Channel dimensions were assessed with a profilometer (Bruker ContourGT, Coventry, UK). The plate used as a fiber holder was laser cut out of 6 mm thick PMMA. Standard fittings (P-221, Upchurch Scientific, WA, USA) were used to attach polytetrafluoroethylene tubing (PTFE, ID 0.75 mm; VWR International Ltd, UK).

2.2 Fabrication of pH sensors

The pH sensors consisted of 10% HydroMed D4 (AdvanSource, MA, USA), 0.1% w/w of a pH dye and 10% Egyptian blue reference particles ($CaCuSi_4O_{10}$) that were produced according to Berke [28], all dissolved and suspended in tetrahydrofuran (THF). Two different pH dyes were employed; dyes number 1 and 3 as presented by Strobl et al. [14] were used for the range of pH 3.5 to pH 6.0 and pH 5.0 to pH 8.5, respectively. The pH sensors were integrated into the reactors using a microdispensing unit (MDC 3200+, MDV 3200A-HS-UF (Vermes, Germany). The dispensing unit included a tappet rod (TTF 20, Vermes, Germany) and nozzle inserts N11-200 (Vermes, Germany). The sensors were dispensed/spotted at the desired position using a 3-axis high performance microstep driver (Triple BEAST), three axis 55 V, 5 A (Controller) (Programmed via LinuxCNC). The microdispenser was controlled with a LabVIEW program (National Instruments Corporation Ltd, Newbury, Berkshire, UK). Repeated application of the sensor compounds to the same location ensured a high fluorophore content at each spot and good signal strength.

2.3 Measurement setup for pH sensors

Two FirestingO_2, (four-channel phase-shift fluorimeters, Pyro Science GmbH, Germany) were used in combination with optical fibers (1 m length, Pyro Science GmbH, Germany) which were held in place by a precisely fitted 6 mm PMMA plate with 2.5 mm diameter holes above the sensor spots. The plate was held in place by slotting into the connector bars. The sensors were read out once per second for a measurement time of 10 ms at an amplitude of 400 mV and a modulation frequency of 2 kHz. Tris-HCl buffer solutions with pH values ranging from pH 3.5 to pH 9.0 were pumped through the μSER at the same flow rate as the reactants. A Boltzmann curve was fitted to the calibration points with OriginPro 9.1 (OriginLab Corporation, China). Before use, pH sensors were conditioned in 50 mM Tris buffer pH 7.0 for 1 h at 10 μL min^{-1}.

2.4 Transketolase production and activity determination

Transketolase (WT-TK from *E. coli* BL21gold DE3 producing plasmid pQR791) was produced in-house according to Matosevic et al. [29] and stored at –80°C in LB medium containing 50% v/v glycerol. Overnight cultures were prepared in 10 g L^{-1} LB medium supplemented with 150 μg mL^{-1} ampicillin and 10 g L^{-1} glycerol. Cells were sub-cultured using 1% v/v inoculum in 2 L shaken flasks containing 500 mL of the supplemented LB broth at 37°C and 250 rpm until the bacterial growth reached stationary phase. Cells were harvested by centrifugation. The cell pellets were resuspended in 50 mM Tris-HCl (Sigma-Aldrich, Gillingham, UK) pH 7.0 and sonicated on ice (Soniprep 150, MSE Sanyo, Japan). The suspension was centrifuged at 13 000 rpm and 4°C for 20 min and filtered afterwards through a 0.2 μm syringe filter (Millipore, US). The lysates were stored at -20°C.

Enzyme activity was determined by mixing 250 μL of a 100 mM lithium-β-hydroxypyruvate (HPA) and 100 mM glycolaldehyde (GA) solution with 250 μL of a transketolase lysate solution (250 μL of TK lysate, 4.8 mM thiamine diphosphate ThDP and 19.6 mM magnesium chloride $MgCl_2$). Both solutions were prepared in 50 mM Tris-HCl buffer pH 7.0. The solutions were incubated at 22°C for 30 min. A volume of 30 μL was removed at one-minute intervals for 3 min and quenched with 270 μL 0.1% v/v

trifluoroacetic acid (TFA), centrifuged (5000 rpm, 5 min) and the supernatant analyzed by HPLC. One transketolase activity unit (U) was defined as the amount of transketolase that catalyzes the conversion of 1 µmol of substrate per minute at pH 7.0 and 20°C.

2.5 Transketolase-catalyzed reaction in the microfluidic side-entry reactor (µSER)

All enzyme and substrate solutions had a starting pH of 7.0 and were pumped using a syringe drive pump (KDS210, KD Scientific, Holliston, US). Samples were taken after three (mean) residence times and 0.1% v/v TFA was added at a 1:10 ratio to quench the reaction.

When using the primary inputs only, equimolar substrate solutions of HPA and GA (from 100 to 500 mM each) and transketolase with an activity of 3.2 U mL^{-1} were used. Substrate and enzyme solutions were inputted at a flow rate ratio of 1:1, yielding a total flow rate of 10 µL min^{-1}. The transketolase was incubated with cofactor concentrations of 2.4 mM ThDP and 9.8 mM $MgCl_2$ for 1 h. The reactions were performed at room temperature.

For the side-entry operation mode, the reactions were performed using a solution containing 600 mM HPA and 100 mM GA for the primary input 2, while the side-entries were supplied from a 500 mM GA solution.

2.6 Penicillin acylase-catalyzed reaction in the microfluidic side-entry reactor (µSER)

Penicillin G acylase (PGA) was purchased from Sigma Aldrich (UK). The reagent and enzyme were prepared in 50 mM Tris-HCl pH 7.0 buffer. Samples were taken at the outlet of the reactor for the colorimetric assay to determine the product concentration. When pH adjustment of the reaction was performed, the side-entries were used to add 50 mM Tris buffers of pH 8.0 and pH 7.5 into the reaction. When using the primary inputs only, the enzyme solution was pumped at the same flow rates as the substrate solution. 20 mM penicillin G (final concentration in reactor) was used to test the conversion and the pH distribution in the µSER. For the side-entry operation mode, a solution of 70 mM penicillin G was added via the side-entries at a flow rate of 0.5 µL min^{-1}, while the enzyme with an activity of 3.3 U mL^{-1} and an initial substrate concentration of 40 mM were pumped in through the primary inputs at a flow rate of 3.5 µL min^{-1}.

2.7 Analytics

2.7.1 Transketolase substrate and product quantification

L-erythrulose (ERY) and HPA were quantified with HPLC (Ultimate 3000 Quarternary Rapid Separation System, Thermo Scientific, UK), using an Aminex HPX-87H column (300 mm × 7.8 mm; Bio-Rad, UK) at 60°C with 0.6 mL min^{-1} isocratic flow and detection at 210 nm. The mobile phase was composed of 0.1% v/v (TFA).

2.7.2 Colorimetric assay for the detection of 6-amino benzyl penicillanic acid (6-APA)

The activity determination for PGA as well as the quantification of 6-APA were performed according to Balasingham et al. [30]. Briefly, 25 µL of sample were pipetted into 175 µL of a derivatizing solution. The derivatizing solution was prepared by adding 0.5 mL of 0.5% w/v p-dimethylaminobenzaldehyde in methanol to 2 mL of 20% acetic acid v/v and 1 mL of 0.05 M NaOH. The reaction of the analyte with the derivatizing solution leads to the formation of a Schiff base, the absorbance of which was measured using a Magellan plate reader (Tecan, Männedorf, Switzerland) at 415 nm.

2.7.3 Statistics

For each condition of the reaction, i.e. for each flow rate, the measurements were conducted as follows: to ensure the measurement occurred when the microfluidic reactor was in steady state, measurements were taken after three (mean) residence times (Supporting information, Fig. S1 and S2). For the pH value at each sensor position, the average from 20 measurements was calculated. The product from each reaction was quantified off-line; the average of three samples was calculated.

All experiments were performed in triplicates, i.e. each flow reaction condition was run three times in separate experiments. The data presented in the graphs are shown as averages of these three repeats. The error bars represent the standard deviation above the mean of three replicate experiments.

3 Results and discussion

3.1 Design of the microfluidic side-entry reactor (µSER)

To demonstrate pH monitoring and reaction condition adjustment in a microfluidic reactor, we re-designed a previously developed microfluidic side-entry reactor [27]. In this previous work, additional inputs of substrate along the reaction channel (we referred to them as auxiliary inputs as opposed to the main inputs at the start of the reaction channel) were used to increase the output concentration. The device however did not contain any online monitoring. For this work, we reduced the number of layers from three to two, and the reaction channel was machined into one of the layers only. This reduction by one layer facilitated optical access to the reaction channel from the top of the reactor which aided the read-out of the sensors integrated in the reactor. Conversely, the total volume of the reactor shrank from 1650 to 550 µL, partially also due to the smaller dimensions of the channel

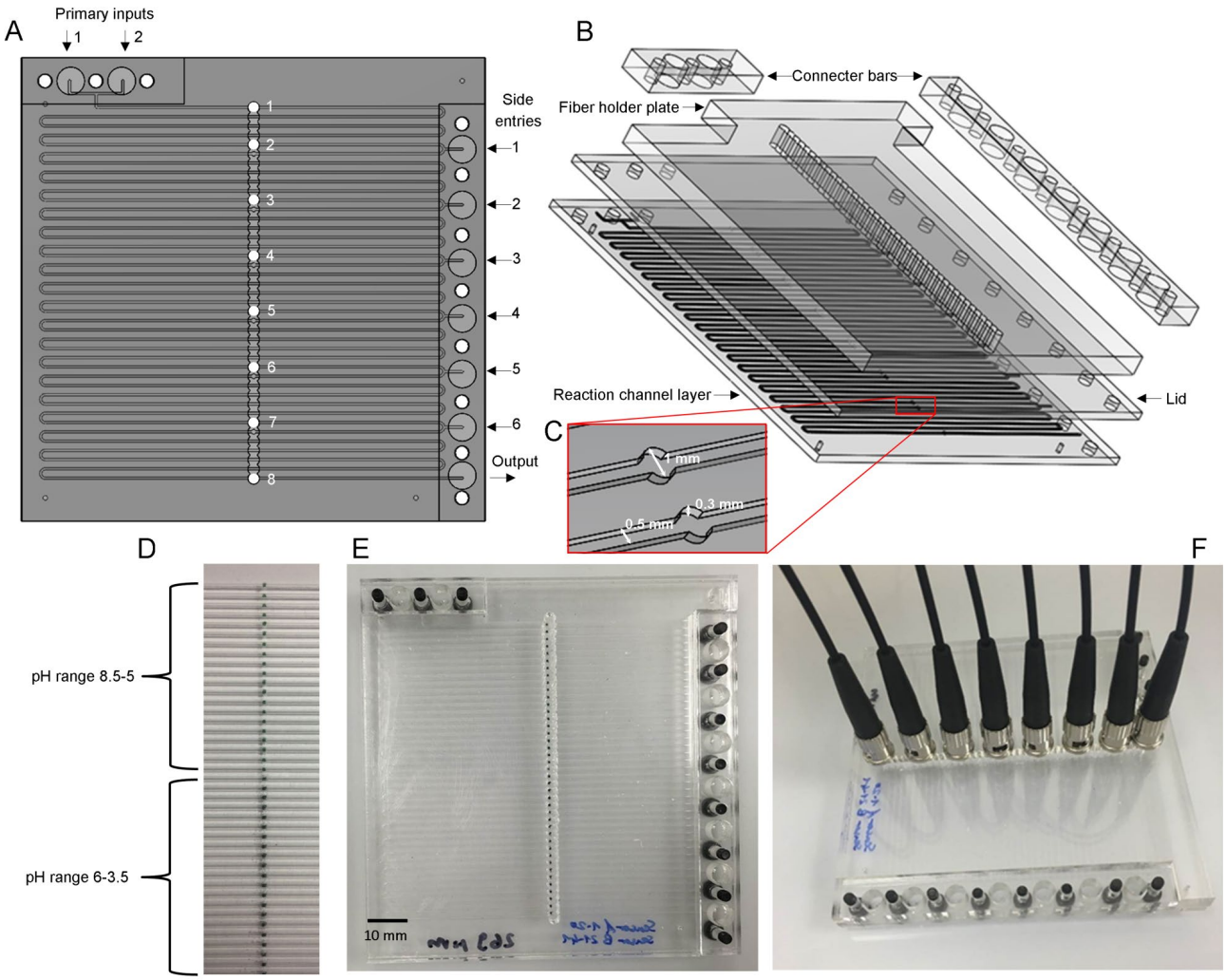

Figure 1. (**A**) Schematic top view representation of the microfluidic side-entry reactor (μSER) with a meandering reaction channel, two primary inputs, six side entry inputs, and a single output. The schematic also shows the eight positions where the pH was monitored. The reactor was operated in two ways: (**i**) using the primary inputs only, i.e. with the six side entry inputs closed, (**ii**) or in 'side entry mode', i.e. with additional substrate or additional pH buffer introduced in all or in a subset of the six side entry inputs. (**B**) Exploded view of the μSER with the reaction channel layer that contained the microfluidic reaction channel, the lid layer which enclosed the channel, the fiber holder plate and the two connector bars. (**C**) Detail view of the reaction channel (300 μm deep and 500 μm wide) and two sensor chambers (diameter of 1 mm). (**D**) Photograph of the sensor array in the μSER consisting of the sensor spots to detect pH between pH 8.5 and 5, and the sensor spots for a pH between 6 and 3.5 in the top and bottom half of the reactor, respectively. (**E**) Photograph of the assembled μSER with the sensor spot array in the center of the photograph (scale bar 10 mm). (**F**) Photograph of the μSER with the fibers for the pH sensor read-out held in the slots of the fiber holder plate. The slots corresponded to the sensor positions 1 to 8 shown in the schematic representation of A.

(300 μm deep and 500 μm wide for this reactor); the narrower channel dimensions were chosen to demonstrate integration of optical sensors in microfluidic channels. Also, the number of side-entries decreased from ten to six. Similar to the previous design, the side-entries were spaced evenly along the reaction channel (yielding equal reaction volumes of ≈90 μL in between each of the inputs), and the reactor was laser machined out of poly(methylmethacrylate) (PMMA). The same type of interconnect bars were used, which can easily be fabricated out of PMMA [31]. Fabrication, bonding, and assembly of the reactor was achieved within 2 h (excluding the time needed for sensor integration).

To monitor pH, optical pH sensors were dispensed into the reaction channel layer of the μSER (Fig. 1) prior to device bonding. At fourteen locations along the reaction channel, a round 'sensor chamber' was machined (diameter of 1 mm) with the same depth as the channel, and the pH sensors were dispensed into the centre of this chamber using a microdispenser. This is a significant reduction in size compared with the use of commercially available sensor spots which are typically available in spot sizes of

3 mm in diameter or larger [32, 33]. In total, 41 sensors were dispensed in the entire reaction channel (14 in the sensor chambers, and 27 outside of the sensor chambers). The sensors had a diameter of 500 µm and a height of 30 µm (Supporting information, Fig. S3) and had a short response time (Supporting information, Fig. S4). For the read-out of the sensors, optical fibers were connected to the µSER using a bespoke fiber holding plate. This plate snugly fitted around the connector bars, which were attached with screws to the microfluidic reactor. As a result, the fiber holder stayed firmly in place once inserted between these bars, and fibers mounted to the fiber holding plate automatically aligned with the pH sensor spots inside the reaction channel (Supporting information, Fig. S5).

To record a time profile of the pH in the reactions, the following eight positions in the µSER were chosen: the first and the last of the sensor positions, i.e. the first position following the primary inputs and the last one before the output; and one sensor position just before each of the six side-entries. For the transketolase reaction, all sensors in the channel contained a dye which enables the detection of pH in the range between pH 5.0 and pH 8.5. For the penicillin G acylase reaction, we chose the sensor dyes with a detection range between pH 5.0 and pH 8.5 for the first four positions; and for the last four positions, the sensor dyes with a range between pH 3.5 and pH 6.0. Calibration of the sensors was performed after thermal bonding of the device at 110°C for 1 h. The calibration plots for these sensors show a typical sigmoid curve and exhibit a high reproducibility across the four positions for both types of sensor dyes (Supporting information, Fig. S4). Furthermore, both sensor dyes combined offer a broad pH detection range between pH 3.5 and pH 8.5 with a high sensitivity of detection between pH 4.5 and pH 7.5 (Supporting information, Fig. S4). We did not detect any significant difference between the sensors dispensed in the sensor chamber and in the channels. However, we found it difficult to properly calibrate the sensors when the device was bonded using an adhesive foil (Supporting information, Fig. S6).

3.2 Real-time pH monitoring of the transketolase catalyzed reaction

Transketolase is a very well-studied enzyme due to its chiral selectivity which makes it a promising enzyme for the biocatalysis of pharmaceutical precursors [34]. The use of hydroxypyruvate (HPA) as a carbon donor yields carbon dioxide as a side product (Scheme 1A), thereby shifting the reaction equilibrium towards the product side and making it irreversible. Due to the solubility and hydration of carbon dioxide in water and the consumption of a proton H^+ in each catalytic cycle of the transketolase-catalyzed condensation using hydroxypyruvate as donor, a formal equivalent of hydrogen carbonate is released, leading to an increase in the pH of the reaction medium.

To test whether we can monitor a pH increase with the integrated sensors, we performed a set of transketolase-catalyzed reactions in the µSER. For the first set of experiments, we used the primary inputs of the µSER only. The transketolase reactions were performed with equimolar concentrations of glycolaldehyde (GA) and HPA and with three different substrate concentrations (50 mM, 150 mM and 250 mM, for each of the substrates). At the start of the reactions, all reaction components were adjusted to pH 7.0.

As can be seen from Fig. 2A, the pH drops at the start of the reaction (Position 1). Also, the drop in pH is larger for higher initial substrate concentrations. Following this drop, the pH increases between 0.4 pH (50 mM initial substrate concentration), 0.7 pH units (150 mM) and one pH unit (250 mM initial substrate concentration). Despite this apparent correlation, the pH change is strongly dependent on the pH value and salinity of the reaction buffer and any linearity in the increase is coincidental. Whilst the increase in pH was expected, and was in fact previously monitored using a colorimetric method with nitrophenol [35], the initial drop in pH was not reported before. Indeed, Yi et al. [35] did not monitor such an initial decrease of pH, though they only performed the reaction with an initial substrate concentration of 50 mM (for which our results also only showed a very small decrease, < 0.1 pH units). A possible explanation for the drop in pH might be the hydrolysis of the glycolaldehyde dimer [36]. In a separate experiment, we examined the impact of GA on the pH of a buffered solution (without any enzyme) and a drop in pH was monitored (data not shown). This highlights how real-time monitoring of pH can potentially reveal new effects in enzymatic reaction processes.

Offline analysis confirmed the bioconversion of the substrates to L-erythrulose (ERY) during the reaction (Fig. 2B). The mean residence time in the microfluidic reactor was 55 min, yielding full conversion for 50 mM and 150 mM, and 95% conversion for 250 mM initial substrate concentration, respectively. It is also noteworthy, that the higher the pH increase was between position 1 and position 8, the higher the product formation.

We then hypothesized that operating the reactor in 'side entry mode' [27, 37], i.e. by adding GA through the side-entries, might result in a higher yield of ERY and that a higher conversion should be noticeable in a different pH profile. To perform these side-entry experiments, transketolase was introduced to the µSER via the primary input 1, and an initial substrate concentration of 300 mM HPA and 50 mM GA (concentrations in the reactor) were introduced via the primary input 2 (both feeds with a flow rate of 3.5 µL min^{-1} each). Along the reaction channel, a total of 250 mM GA was added using the six side-entries.

In a first experiment, a flow rate of 0.25 µL min^{-1} and in a second experiment a flow rate of 0.5 µL min^{-1} was

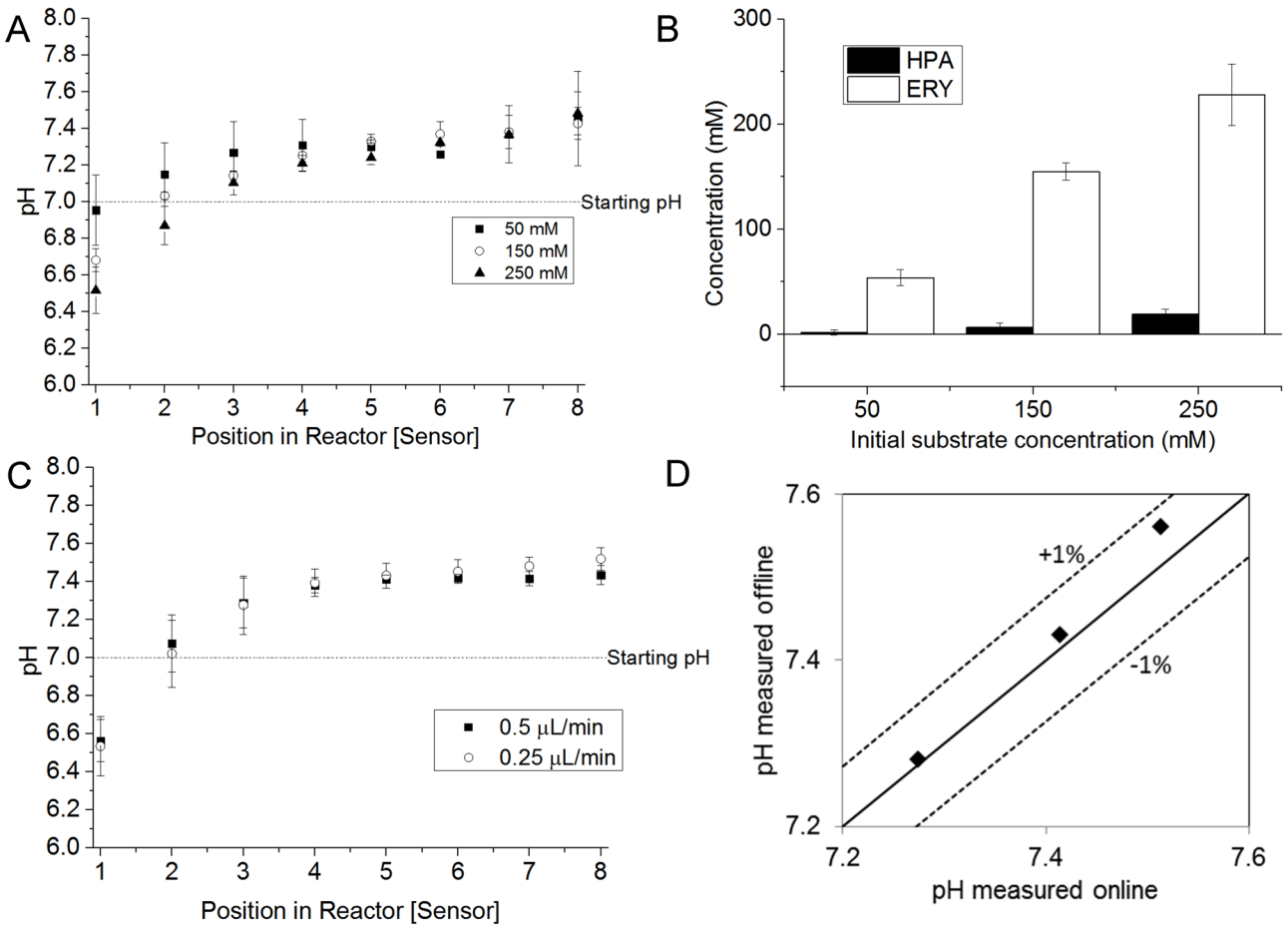

Figure 2. (**A**) pH values for the transketolase-catalyzed reaction monitored at eight positions in the µSER, if operated with the primary inputs only. The results show three flow reactions, each using a different initial substrate concentration (50, 150 and 250 mM), but obtained with the same flow rate of 10 µL min^{-1}. (**B**) The concentrations for the product erythrulose (ERY) and the residual substrate, Li-β-hydroxypyruvate (HPA), measured at the output for the three different flow reactions. (**C**) pH values for the transketolase-catalyzed reaction when operated in side-entry mode. Reactions were performed at two different flow rates for the side-entries (0.25 and 0.5 µL min^{-1}, total flow rates of 8.5 and 10 µL min^{-1}). For both flow rates, the pH increased continuously over the course of the reaction, with a difference between position 1 and position 8 of about one pH unit. Both set of reactions were performed in triplicates, and the data are shown as the average of three runs with the error bars representing one standard deviation. (**D**) Parity plot showing the pH readout of the last sensor in the reactor (Position 8) compared to the readout of an offline pH electrode. The deviation between the two measurement techniques is less than one percent, demonstrating the robustness of the integrated optical sensors.

chosen for the GA inputs. The exact configurations of the inputs for the reaction are summarized in Table 1.

For both flow rates, the pH time profiles showed the same initial drop of pH at the beginning of the reaction, and again a total increase of one pH unit was observed throughout the reaction (Fig. 2C). A total concentration of 220 mM (± 6.5 mM) and 230 mM (± 6.8 mM) ERY was measured at the end of the reaction using 0.5 µL min^{-1} and 0.25 µL min^{-1} as the side-entry flows, respectively. This corresponds to a conversion of approximately 95%.

These experiments thus demonstrated that we can monitor in real time the pH changes in a transketolase-catalyzed reaction. Additionally, the pH sensors are sensitive enough to resolve changes in pH clearly smaller than 0.1 pH units (Fig. 2D), as was confirmed in comparison with offline analysis using a standard electrode. As can be seen from the calibration curves in the Supporting information, Fig. S4, it is very likely that much smaller units of pH can be resolved, but this was not further examined in this work.

At the higher substrate concentrations (250 mM in Fig. 2A and 300 mM in Fig. 2C), we observed the formation of bubbles in the reaction channel which might be due to the formation of carbon dioxide as a side reaction. The bubbles passed through the reactor and did not accumulate in the sensor chambers or above the sensors, and thus did not obstruct pH sensor read-out.

The pH time profiles did not vary significantly when introducing a 250 mM initial substrate concentration at once (using the primary inputs only) or when introducing

Table 1. Initial concentrations and flow rates used for the operation of the transketolase catalyzed reaction in side-entry mode. All solutions were prepared in 50 mM Tris-HCl buffer pH 7.0. The reactions were performed at 22°C. Initial enzyme activity was 3.2 U mL^{-1}.

Input	Substrate concentration at input (mM)	Concentration after mixing (mM)	Flow rate (µL min^{-1})
Primary input 1	Transketolase	Transketolase	3.5
Primary input 2	100 GA + 600 HPA	50 GA + 300 HPA	3.5
Side-entry 1	500 GA	20.75/41.50 GA	0.25/0.5
Side-entry 2	500 GA	20.03/40.06 GA	0.25/0.5
Side-entry 3	500 GA	19.37/38.73 GA	0.25/0.5
Side-entry 4	500 GA	18.74/37.48 GA	0.25/0.5
Side-entry 5	500 GA	18.16/36.31 GA	0.25/0.5
Side-entry 6	500 GA	17.61/35.21 GA	0.25/0.5

a 300 mM initial substrate concentration over several inputs; both reactions showed a pH increase of about one pH unit. Additionally, both sets of experiments yielded a conversion of about 95%. This is thus further indication that real-time availability of a pH time profile could be employed to predict the conversion efficiency of a reaction. This is in agreement with Yi et al. [35] which correlated pH changes with substrate tolerance for TK.

As neither experiments led to a change in the pH to a value outside of the operating range of the TK enzyme, it is unlikely that a control of the pH would have led to a noticeable change in conversion, and thus a pH adjustment was not attempted with this enzyme system.

3.3 Real-time pH monitoring of the penicillin G acylase catalyzed reaction

During the reaction with penicillin G, catalyzed by penicillin G acylase (PGA), two acids, 6-amino benzyl penicillanic acid (6-APA) and phenyl acetic acid (PA), are produced as a result of hydrolysis (Scheme 1B) leading to a pH shift. The acid production can overcome the buffer capacity of the system and drop the pH into a range too low for the enzyme to function. The optimal pH for free PGA from *E. coli* is known to be between pH 6.0 and pH 8.0. [38]

For this reaction, PGA in 50 mM Tris-HCl pH 7.0 buffer was fed via the primary input 1, and 40 mM of penicillin G (i.e. a 20 mM initial concentration in the reactor) in the same buffer via primary input 2; both were fed at the same flow rates. In total, four different flow rates (5, 10, 20 and 40 µL min^{-1} at each inlet of the two, yielding total flow rates of 10, 20, 40 and 80 µL min^{-1}, respectively) were tested. Again, all reaction components were adjusted to pH 7.0 prior to their introduction into the reactor. As can be seen from Fig. 3A, the lower the flow rate, the faster the pH dropped. For all flow rates, approximately the same conversion of substrate was achieved (Fig. 3B).

Two 'side entry' experiments were performed. PGA in a 50 mM Tris-HCl pH 7.0 buffer were fed via the primary input 1, and 5 mM or 10 mM of penicillin G (i.e. a 2.5 or 5 mM initial concentration in the reactor, respectively) in the same buffer via primary input 2; both were fed at a flow rate of 3.5 µL min^{-1}. Via the side-entries, an additional 2.5 mM or 5 mM of substrate were added with a flow rate of 0.5 µL min^{-1}.

In the two-input reaction with 20 mM initial substrate concentration a final product concentration between 6 and 6.9 mM was achieved (Fig. 3B). In the 'side-entry' where a 2.5 mM initial substrate concentration was followed up with six additions of 2.5 mM of penicillin G (hence a total of 16.3 mM, taking dilution effects into account) a final product concentration of 4.4 ± 0.1 mM was detected. A lower amount of substrate thus led to a lower amount of product, which can be expected. However, in the 'side entry' reaction, where a 5 mM initial

Table 2. Initial concentrations and flow rates used for the operation of the penicillin G acylase catalyzed reaction in side-entry mode without pH adjustment. All solutions were prepared in 50 mM Tris-HCl buffer pH 7.0. The reactions were performed at 22°C. Initial enzyme activity was 3.3 U mL^{-1}.

Input	Substrate concentration at input (mM)	Concentration after mixing (mM)	Flow rate (µL min^{-1})
Primary input 1	Penicillin G Acylase	Penicillin G Acylase	3.5
Primary input 2	10/5	5/2.5	3.5
Side-entry 1	35/17.5	5.00/2.50	0.5
Side-entry 2	35/17.5	4.83/2.41	0.5
Side-entry 3	35/17.5	4.67/2.33	0.5
Side-entry 4	35/17.5	4.52/2.26	0.5
Side-entry 5	35/17.5	4.38/2.19	0.5
Side-entry 6	35/17.5	4.24/2.12	0.5

substrate concentration was followed up with six additions of 5 mM of penicillin G (hence a total of 32.6 mM penicillin G, taking dilution effects into account), the final product concentration measured (6.7 ± 0.1 mM) did not exceed the 6.9 mM from the two-input reaction (where a total of 20 mM initial substrate concentration was converted). The exact configurations of the inputs for the reaction are summarized in Table 2. In this reaction, the pH dropped to below pH 4.5. It is therefore likely, that further conversion was either prevented by the significant drop in pH or by a solubility maximum of 6-APA which is estimated to be approximately 12.5 mM [39]. We therefore hypothesized that a higher conversion could be achieved, if the side-entries are employed to adjust the pH during the reaction.

3.4 pH adjustment of the penicillin G acylase reaction

To test the effect of pH adjustment on the overall yield of the penicillin G acylase-catalyzed reaction, an initial substrate concentration of 20 mM in the reactor was added via primary input 2. To demonstrate pH adjustment, reactions were performed with two different sets of flow rates (20 and 40 µL min^{-1}). The reactions were first performed without pH adjustment. This resulted in a pH drop below pH 6.0 within the first half of the reactor. We then demonstrated the possibility of adjusting the pH via the side-entries. This was done by adding buffers of pH 7.5 and 8.0 into the reactor at constant flow rates (steady-state addition). The aim was to keep the pH within the enzyme's optimal operating range, i.e. a pH between 6.0 and 8.0. The exact buffers and input points are listed in Table 3. Two different flow rates for both the primary and side-entries were used to demonstrate the differences that resulted from a change in residence time.

The reactions were first performed without pH adjustment to acquire a pH time course profile for the reaction under these conditions. Using the sensor read-out from these reactions we were able to determine at which point, i.e. for which side-entry pH adjustment should begin. This was determined to be at the sensor position (5) where the pH dropped below 6.0 in the reaction without pH adjustment. Therefore, 50 mM Tris-HCl buffer pH 8.0

Table 3. Initial concentrations and flow rates used for the operation of the penicillin G acylase catalyzed reaction in side-entry mode with pH adjustment. All solutions were prepared in 50 mM Tris-HCl buffer pH 7.0. The reactions were performed at 22°C. Initial enzyme activity was 3.3 U mL^{-1}.

Input	Input	Flow rate (µL min^{-1})
Primary input 1	Penicillin acylase	40/20
Primary input 2	40 mM Penicillin G	40/20
Side-entry 1	Milli Q Water	5/2.5
Side-entry 2	Milli Q Water	5/2.5
Side-entry 3	50 mM TrisHCl pH 8	5/2.5
Side-entry 4	50 mM TrisHCl pH 8	5/2.5
Side-entry 5	50 mM TrisHCl pH 7.5	5/2.5
Side-entry 6	50 mM TrisHCl pH 7.5	5/2.5

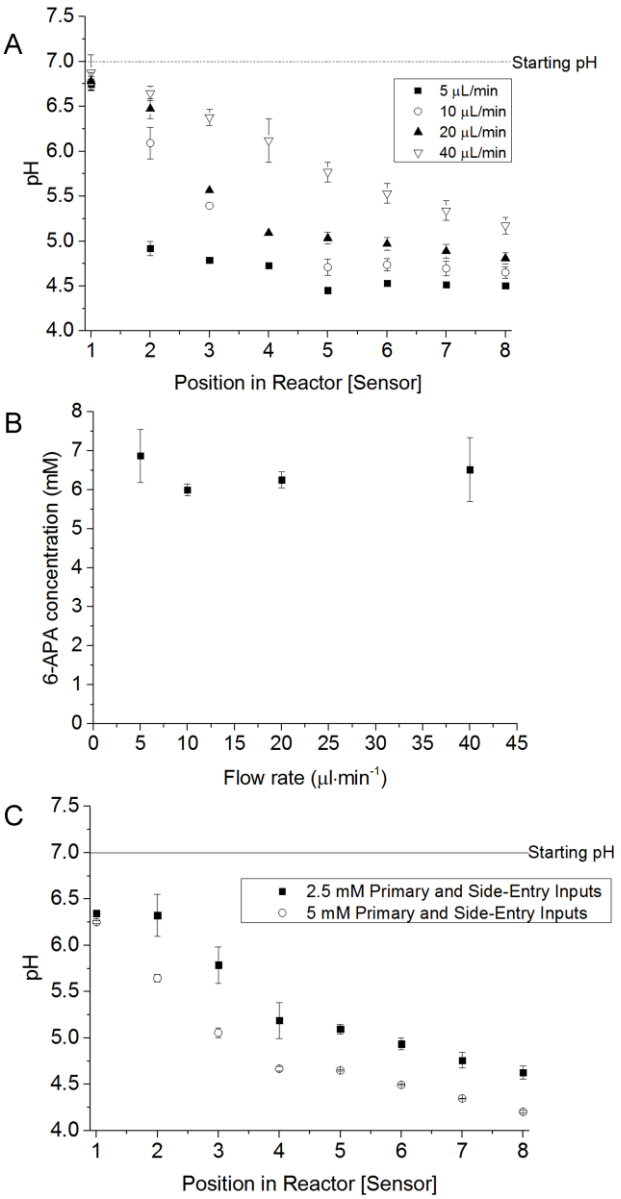

Figure 3. (**A**) pH values of the penicillin G acylase catalyzed reaction performed in 50 mM Tris-buffer pH 7.0 in the µSER. The graph shows that the acid production can overcome the buffer capacity and accordingly tip the pH into a range in which the enzyme is no longer active. The reactions were performed at four different flow rates. (**B**) Concentration of the product 6-amino penicillanic acid (6-APA). The product concentration was measured offline using a colorimetric assay at 415 nm. (**C**) pH values obtained for the penicillin acylase catalyzed reaction when operating the µSER in side-entry mode. The graph shows the results from two experiments, each with a different substrate concentration (2.5 mM and 5 mM). For both substrate concentrations, the pH continuously decreases by about 2.5 pH units over the course of the reaction. Reactions were performed in triplicates, and the data are shown as an average of three runs with the error bars representing one standard deviation.

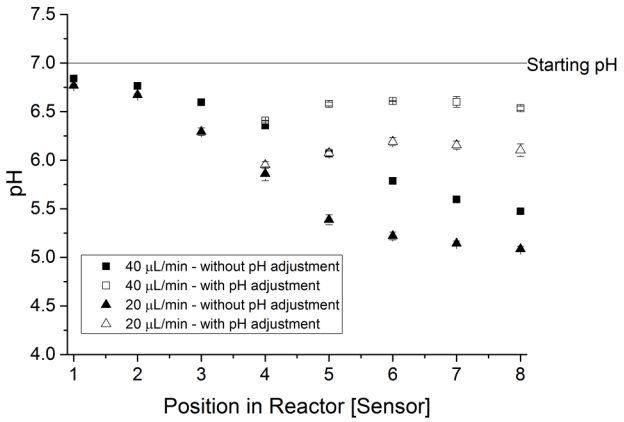

Figure 4. pH profiles of the penicillin G acylase catalyzed reaction in the µSER with and without pH adjustment. To adjust pH, additional buffer was inputted in the side entry inputs number 4, 5 and 6. The results show that the pH of the reaction was maintained above a pH value of 6, i.e. within the enzyme's optimal operating range (pH 6 to 8). Reactions were performed in triplicates, and the data are shown as average of three runs with the error bars representing one standard deviation. For the first three positions, the pH values for the pH adjusted reaction overlap with the values of the un-adjusted reaction, and the first three values of the pH adjusted reaction are therefore omitted from the graph for better legibility.

was added via auxiliary inlet 3 and 4 and 50 mM Tris-HCl buffer pH 7.5 was added via side-entries 5 and 6.

As can be seen from Fig. 4, with pH adjustment, the pH in the system was maintained above pH 6.0, which likely promoted a better stability of the enzyme. This kept the reaction conditions within an optimal range for the enzyme and resulted in higher yields. Without pH adjustment, a product concentration of 7.2 ± 0.2 mM was achieved with the 20 µL min^{-1} flow rate, and 7.1 ± 0.5 mM with the 40 µL min^{-1} flow rate. With pH adjustment, a product concentration of 6.7 ± 0.3 mM for the slower flow rate and a final concentration of 5.9 ± 0.3 mM for the faster flow rate was attained. When corrected for dilution, a concentration of 9.3 mM for the pH adjusted 20 µL min^{-1} reaction and a concentration of 8.1 mM for the 40 µL min^{-1} reaction was obtained, resulting in a yield increase of 29% and 14%, respectively. For product recovery, the dilution of the product during the reaction step could lead to an increase in the costs downstream.

4 Conclusion

We developed a novel microfluidic side-entry reactor (µSER) with integrated optical pH sensors. Using two types of optical sensors, each with a different dye, the reactor was capable of detecting pH between 3.5 and 8.5 which is a broader range than typically reported. A sensor calibration performed after the thermal bonding of the µSER showed high reproducibility over the entire detection range, and proved that the sensors are heat stable to sustain the temperatures typical for thermal bonding of microfluidic devices. This robustness greatly facilitates their integration into enclosed microfluidic devices. Furthermore, by monitoring the pH at eight different positions in the reactor, we were able to obtain time-course profiles of the pH for enzymatic reactions.

The µSER was validated with two industrially relevant enzymatic reactions, a transketolase- and a penicillin G acylase-catalyzed reaction, and we successfully demonstrated real-time pH monitoring and establishment of pH time-course profiles for both reactions. Without pH adjustment, the transketolase-catalyzed reaction showed a pH increase of one pH unit and the penicillin G acylase-catalyzed reaction a pH decrease of approximately 2.5 pH units. When comparing the differences in pH units between the first and last sensor position for the TK-catalyzed reaction, the increase of L-erythrulose produced was clearly met by a change in pH. The pH change thus also provided a first indication of the level of conversion that is being achieved in the reactor, i.e. real-time information on the reaction progress.

The µSER contained fluidic inputs, i.e. side entries, along the reaction channel which were used to adjust the pH of the reaction. With pH adjustment, the pH drop of the penicillin G acylase-catalyzed reaction was significantly attenuated. As a result, the reaction condition was kept at a pH suitable for the operation of the enzyme, and the product yield significantly increased.

We have therefore shown that a detailed knowledge of the time-course profile of a reaction can be used to optimize the reaction conditions of an enzymatic reaction, highlighting the potential of instrumented microfluidic reactors for process development. The importance of online monitoring has been described among the development needs for microbioreactors [40, 41], and time-course profiles of process parameters have been shown for fermentation [42] and stem cell culture [43]. Therefore, further applications of this approach are not only of interest for analytical and synthetic enzymatic reactions, enzyme stability studies or bioprocess development, but for a variety of biotechnological applications where continuous flow microreactors can be envisioned.

The authors gratefully acknowledge the People Programme (Marie Curie Actions, Multi-ITN) of the European Union's Seventh Framework Programme for research, technological development and demonstration, for funding Pia Gruber's PhD studentship (Grant Number 608104) and the Biotechnology and Biological Sciences Research Council (BBSRC, BB/L000997/1). We thank Manni Bhatti (UCL) for her support with redacting of this manuscript.

The authors declare no financial or commercial conflict of interest.

5 References

[1] Cornish-Bowden, A., *Fundamentals of Enzyme Kinetics*, 3rd Edn., Portland Press 2004, pp. 213–228.
[2] Jacobsen, C., Leonis, J., Linderstrøm-Lang, K., Ottesen, M., The pH-stat and its use in biochemistry. *Methods Biochem. Anal.* 1957, *4*, 171–210.
[3] Bergveld P., Development, operation, and application of the ion-sensitive field-effect transistor as a tool for electrophysiology. *IEEE Trans. Biomed. Eng.* 1972, *19*, 342–351.
[4] Schasfoort, R. B., Field-effect flow control for microfabricated fluidic networks. *Science* 1999, *286*, 942–945.
[5] Sharma, S., Moniz, A., Triantis, I., Michelakis, K. et al., An integrated silicon sensor with microfluidic chip for monitoring potassium and pH. *Microfluid. Nanofluid.* 2010, *10*, 1119–1125.
[6] Welch, D.Christen, J., Real-time feedback control of pH within microfluidics using integrated sensing and actuation. *Lab Chip* 2014, *14*, 1191.
[7] Kirk, T.Szita, N., Oxygen transfer characteristics of miniaturized bioreactor systems. *Biotechnol. Bioeng.* 2013, *110*, 1005–1019.
[8] Liebsch, G., Klimant, I., Krause, C., Wolfbeis, O., Fluorescent imaging of pH with optical sensors using time domain dual lifetime referencing. *Anal. Chem.* 2001, *73*, 4354–4363.
[9] Jezierski, S., Belder, D., Nagl, S., Microfluidic free-flow electrophoresis chips with an integrated fluorescent sensor layer for real time pH imaging in isoelectric focusing. *Chem. Commun.* 2013, *49*, 904–906.
[10] Funfak, A., Cao, J., Wolfbeis, O., Martin, K., Köhler, J., Monitoring cell cultivation in microfluidic segments by optical pH sensing with a micro flow-through fluorometer using dye-doped polymer particles. *Microchim. Acta* 2008, *164*, 279–286.
[11] Lee, K., Boccazzi, P., Sinskey, A., Ram, R., Microfluidic chemostat and turbidostat with flow rate, oxygen, and temperature control for dynamic continuous culture. *Lab Chip* 2011, *11*, 1730.
[12] Ehgartner, J., Strobl, M., Bolivar, J., Rabl, D. et al., Simultaneous determination of oxygen and pH inside microfluidic devices using core-shell nanosensors. *Anal. Chem.* 2016, *88*, 9796–9804.
[13] Mousavi Shaegh, S., De Ferrari, F., Zhang, Y., Nabavinia, M. et al., A microfluidic optical platform for real-time monitoring of pH and oxygen in microfluidic bioreactors and organ-on-chip devices. *Biomicrofluidics* 2016, *10*, 044111.
[14] Strobl, M., Rappitsch, T., Borisov, S., Mayr, T., Klimant, I., NIR-emitting aza-BODIPY dyes – new building blocks for broad-range optical pH sensors. *Analyst* 2015, *140*, 7150–7153.
[15] Bruggink, A., Roos, E.C., de Vroom, E., Penicillin acylase in the industrial production of β-lactam antibiotics. *Org. Process Res. Dev.* 1998, *2*, 128–133.
[16] Franssen, M. C. R., Kircher, M., Wohlgemuth, R., Industrial biotechnology in the chemical and pharmaceutical industries, in: Soetaert, W., Vandamme, E. J. (Eds.), *Industrial Biotechnology. Sustainable Growth and Economic Success*, Wiley-VCH Verlag GmbH & Co. KGaA, Weinheim, Germany 2010, pp. 323–351
[17] Buchholz, K., A breakthrough in enzyme technology to fight penicillin resistance – industrial application of penicillin amidase. *Appl. Microbiol. Biotechnol.* 2016, *100*, 3825–3839.
[18] Srirangan, K., Orr, V., Akawi, L., Westbrook, A. et al., Biotechnological advances on penicillin G acylase: pharmaceutical implications, unique expression mechanism and production strategies. *Biotechnol. Adv.* 2013, *31*, 1319–1332.
[19] Hecquet, L., Fessner, W., Hélaine, V., Charmantray, F., New applications of transketolase: Cascade reactions for assay development, in: Riva, S., Fessner, W.-D. (Eds.), *Casacade Biocatalysis: Integrating Stereoselective and Environmentally Friendly Reactions*, Wiley-VCH Verlag GmbH & Co. KGaA, Weinheim, Germany 2014, 315–338.
[20] (a) Ingram, C. U., Bommer, M., Smith, M. E. B., Dalby, P. A. et al., One-pot synthesis of amino-alcohols using a de-novo transketolase and β-alanine:pyruvate transaminase pathway in *Escherichia coli*. *Biotechnol. Bioeng.* 2007, *96*, 559–569. (b) Slovejeva, O. N., Kochetov, G. A. *J. Mol. Catal. B: Enzym.* 2008, *54*, 90–92. (c) Charmantray, F., Helaine, V., Legeret, B., Hecquet, L., *J. Mol. Catal. B: Enzym.* 2009, *57*, 6–9.
[21] Wohlgemuth, R., Smith, M. E., Dalby, P. A., Woodley, J. M., Transketolases, in: *Encyclopedia of Industrial Biotechnology*, John Wiley & Sons 2009, pp. 1–7.
[22] Hobbs, G. R., Lilly, M. D., Turner, N. J., Ward, J. M. et al., Enzyme catalysed carbon-carbon bond formation: use of transketolase from *Escherichia coli*. *J. Chem. Soc., Perkin Trans.* 1993, *1*, 165–166.
[23] Mitra, R. K., Woodley, J. M., A useful assay for transketolase inasymmetric syntheses. *Biotechnol. Tech.* 1996, *10*, 167–172.
[24] Shaeri, J., Wohlgemuth, R., Woodley, J. M., Semiquantitative process screening for the biocatalytic synthesis of D-xylulose 5-phosphate. *Org. Process Res. Dev.* 2006, *10*, 605–610.
[25] Shaeri, J., Wright, I., Rathbone, E.B., Wohlgemuth, R. Woodley, J.M., Characterization of enzymatic D-xylulose 5-phosphate synthesis. *Biotechnol. Bioeng.* 2008, *101*, 761–767.
[26] Boniello, C., Mayr, T., Bolivar, J., Nidetzky, B., Dual-lifetime referencing (DLR): A powerful method for on-line measurement of internal pH in carrier-bound immobilized biocatalysts. *BMC Biotechnol.* 2012, *12*, 11.
[27] Lawrence, J., O'Sullivan, B., Lye, G., Wohlgemuth, R., Szita, N., Microfluidic multi-input reactor for biocatalytic synthesis using transketolase. *J. Mol. Catal. B: Enzym.* 2013, *95*, 111–117.
[28] Berke, H., The invention of blue and purple pigments in ancient times. *Chem. Soc. Rev.* 2007, *36*, 15–30.
[29] Matosevic, S., Micheletti, M., Woodley, J.M., Lye, G.J., Baganz, F., Quantification of kinetics for enzyme-catalysed reactions: implications for diffusional limitations at the 10 ml scale. *Biotechnol. Lett.* 2008, *30*, 995–1000.
[30] Balasingham, K., Warburton, D., Dunnill, P., Lilly, M., The isolation and kinetics of penicillin amidase from *Escherichia coli*. *Biochim. Biophys. Acta, Enzymol.* 1972, *276*, 250–256.
[31] Reichen, M., Super, A., Davies, M. J., Macown, R. J. et al. Characterisation of an adhesive-free packaging system for polymeric microfluidic biochemical devices and reactors. *ChemBioChem* 2014, *28*, 189–202.
[32] Ocean optics weblink (accessed 25.07.2016): http://oceanoptics.com/product/ph-bcg-trans/
[33] PreSens weblink (accessed 25.07.2016): http://www.presens.de/products/brochures/category/sensor-probes/brochure/non-invasive-ph-sensors.html
[34] Wohlgemuth, R., C2-Ketol elongation by transketolase-catalyzed asymmetric synthesis. *J. Mol. Catal. B: Enzym.* 2009, *61*, 23–29.
[35] Yi, D., Devamani, T., Abdoul-Zabar, J., Charmantray, F. et al., A pH-based high-throughput assay for transketolase: Fingerprinting of substrate tolerance and quantitative kinetics. *ChemBioChem* 2012, *13*, 2290–2300.
[36] Bell, R. P, Hirst, J. P. H., Acid-base catalysis in the depolymerisation of dimeric glycolaldehyde. *J. Chem. Soc.* 1939, 1777–1780.
[37] Cervera-Padrell, A., Nielsen, J., Jønch Pedersen, M., Müller Christensen, K. et al., Monitoring and control of a continuous Grignard reaction for the synthesis of an active pharmaceutical ingredient intermediate using inline NIR spectroscopy. *Org. Process Res. Dev.* 2012, *16*, 901–914.
[38] Zuza, M., Siler-Marinkovic, S., Knezevic, Z., Immobilization of penicillin acylase from *Escherichia coli* on commercial sepabeads EC-EP carrier. *Acta Per Tech.* 2007, 173–182. doi: 10.2298/APT0738173Z.

[39] Sigma Aldrich, (+)-6-Aminopenicillanic acid Safety Data Sheet, No. 1907/2006, Version 5.0 Revision Date 08.01.2013, Print Date 13.12.2016.
[40] Gernaey, K. V., Baganz, F., Franco-Lara, E., Kensy, F. et al., Monitoring and control of microbioreactors: An expert opinion on development needs. *Biotechnol. J.* 2012, *7*, 1308–1314.
[41] Kirk, T., Szita, N., Oxygen transfer characteristics of miniaturized bioreactor systems. *Biotechnol. Bioeng.* 2013, *110*, 1005–1019.
[42] Zanzotto, A., Szita, N., Boccazzi, P., Lessard, P. et al., Membrane-aerated microbioreactor for high-throughput bioprocessing. *Biotechnol. Bioeng.* 2004, *87*, 243–254.
[43] Super, A., Jaccard, N., Cardoso Marques, M., Macown, R. et al., Real-time monitoring of specific oxygen uptake rates of embryonic stem cells in a microfluidic cell culture device. *Biotechnol. J.* 2016, *11*, 1179–1189.